Optica Applicata, Vol. XLVI, No. 4, 2016
DOI: 10.5277/oa160412

Disparity servoing based fast autofocusing method for stereomicroscope

YI LIU[1], MEI YU[1*], LI CUI[1], GANGYI JIANG[1], YIGANG WANG[1, 2], SHENGLI FAN[1, 2]

[1]Department of Information Science and Engineering, Ningbo University, Ningbo, China

[2]Department of Information, Ningbo Institute of Technology, Zhejiang University, Ningbo, China

[*]Corresponding author: yumei2@126.com

A disparity servoing based fast autofocusing method is proposed for stereomicroscopes according to linear relationship between the disparity change in stereomicroscopic images and the move distance of a motorized translation stage. For a certain stereomicroscope, the calibration of a disparity range of clear images at each magnification is implemented offline. After that, the disparity of the stereomicroscopic image is used as an index to represent the sharpness of an arbitrary image. If the disparity does not satisfy the requirement, move steps and direction of a step motor are calculated by utilizing the linear relationship between the disparity change and the move distance of the stage. The iteration will be continued until the disparity of the captured stereomicroscopic image approximates to the clearest disparity. The experimental results show that the proposed method only requires a few iterations and less time to reach the focus position, and the disparity error is less than 0.5 pixel.

Keywords: autofocusing, stereomicroscope, stereomicroscopic images, disparity.

1. Introduction

Machine vision systems are widely used in the field of micromanipulation and inspection [1, 2], because of their reliability, relatively lower price, and high throughput. To implement such systems, the sharpness of images captured by a camera should be guaranteed. In the automatic industry and in biomedical applications, such as high throughput screening in manufacturing industry and microcell injection, autofocusing is one of the fundamental techniques [3]. In a routine microscope use, such as in the micro-assembling of microelectromechanical systems (MEMS) [4], fast stable autofocusing methods are indispensable.

In visual systems, focusing helps obtain the clearest image from a series of images by adjusting the objective. Autofocusing methods are classified into active and passive types [5]. Active methods detect and adjust the distance between the object and camera by using different transmitting equipment, such as infrared and ultrasonic generators.

In contrast, passive methods select the clearest image by analyzing information from a series of images.

Most traditional autofocusing methods first select an optimal sharpness function, and then choose an image with the maximum sharpness function value as the focus image through inputting a series of images with different focal distances. Different sharpness functions have been studied for evaluating image sharpness [6, 7]. YU SUN *et al*. contrasted 18 existing sharpness functions under different conditions, and two robust sharpness functions were obtained [6]. BARAN *et al*. proposed a self-optimizing structure to realize autofocusing by analyzing the relationship of magnification and focus position of microscopic system [8]. With regard to microscopic systems, it is time-consuming to move at fixed steps to capture a series of images under each magnification. For solving this problem, many autofocusing methods have been proposed based on optical theory [9, 10]. MARTURI *et al*. also proposed a fast robust autofocusing method based on visual servoing in scanning microscopic systems [11].

This paper proposes a disparity servoing based fast autofocusing algorithm for stereomicroscopes. The proposed algorithm chooses the disparity of stereomicroscopic images as an index to represent the sharpness of stereomicroscopic images. In addition, according to the relationship between the disparity of stereomicroscopic images and the height of the motorized translation stage, the algorithm cannot only judge the sharpness of an arbitrary microscopic image, but also calculate the move steps and direction of the step motor to reach the focus position.

2. Disparity servoing based fast autofocusing method

For a monocular microscope, it is difficult to judge whether an arbitrary image is clear enough to satisfy the requirement if there are no other reference images. Thus, for most traditional autofocusing methods, it needs to capture a series of images from blurry to clear and back to blurry again so as to choose the clearest one from those images by comparing their sharpness function values. Since the magnitude of sharpness function relates to the content of the image and magnification of the microscope, the above time consuming process has to be implemented for each final obtained clearest image. However, this is different for a stereomicroscope, since there is useful information called disparity relating to the sharpness of a stereomicroscopic image benefiting from its relationship with the distance between the object and the cameras.

2.1. Relationship between disparity of stereomicroscopic image and height of motorized translation stage

Figure 1 shows a schematic of the binocular imaging of stereomicroscopes, where J_L and J_R represent the convex lenses of the left and right cameras, respectively; X_L and X_R denote the left and right imaging planes, respectively; α_L denotes the angle between the motorized translation stage T and the left imaging plane, and α_R denotes

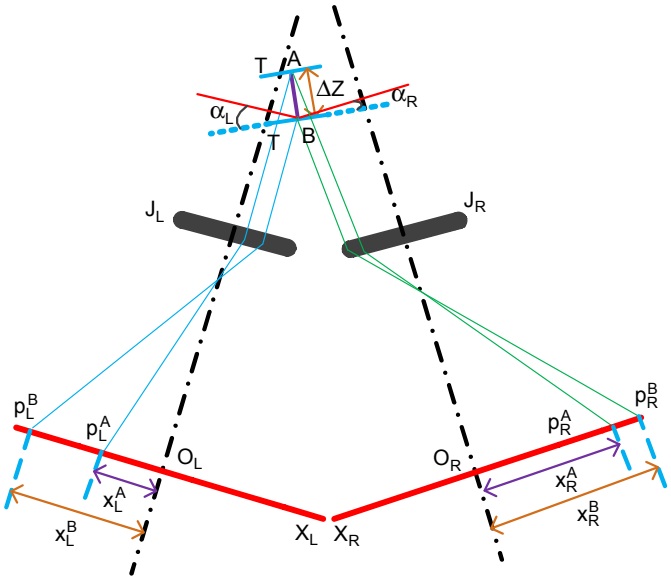

Fig. 1. Schematic diagram of binocular imaging of stereomicroscope (see text for explanation).

the angle between the T and the right imaging plane; the dash-dot lines across the points O_L and O_R are the optic axes of the left and right cameras, respectively; β_L and β_R are the magnification of the two cameras, respectively. The distance between the object and the cameras of the stereomicroscope is determined by the height of a motorized translation stage because the object is placed on the stage. A 3D point A exists on the motorized translation stage T, and if this point is moved along with the motorized translation stage with a move distance ΔZ, it will reach another 3D point B. Further, $p_L^A(x_L^A, y_L^A)$ and $p_R^A(x_R^A, y_R^A)$ are the respective image coordinates of point A imaging on X_L and X_R, while $p_L^B(x_L^B, y_L^B)$ and $p_R^B(x_R^B, y_R^B)$ are the respective image coordinates of point B imaging on X_L and X_R.

According to the imaging principle of a telecentric lens, the following equation can be expressed with geometry knowledge

$$\begin{cases} x_L^A = \beta_L x_l \\ x_R^A = \beta_R x_r \\ x_L^B = \beta_L [x_l + \Delta Z \sin(\alpha_L)] \\ x_R^B = \beta_R [x_r + \Delta Z \sin(\alpha_R)] \end{cases} \tag{1}$$

where x_l and x_r represent the distance from point A to the left and right optical axes, respectively; and $[x_l + \Delta Z\sin(\alpha_L)]$ and $[x_r + \Delta Z\sin(\alpha_R)]$ represent the distance from

point B to the left and right optical axes, respectively. Let d_A and d_B be the disparities of points A and B in corresponding stereomicroscopic images, calculated by

$$\begin{cases} d_A = x_{\mathrm{L}}^A - (-x_{\mathrm{R}}^A) = \beta_{\mathrm{L}} x_{\mathrm{l}} + \beta_{\mathrm{R}} x_{\mathrm{r}} \\ d_B = x_{\mathrm{L}}^B - (-x_{\mathrm{R}}^B) = \beta_{\mathrm{L}}[x_{\mathrm{l}} + \Delta Z \sin(\alpha_{\mathrm{L}})] + \beta_{\mathrm{R}}[x_{\mathrm{r}} + \Delta Z \sin(\alpha_{\mathrm{R}})] \end{cases} \tag{2}$$

The change Δd in disparity when the motorized translation stage T moves from point A to point B can be inferred as follows:

$$\Delta d = d_B - d_A = \beta_{\mathrm{L}} \Delta Z \sin(\alpha_{\mathrm{L}}) + \beta_{\mathrm{R}} \Delta Z \sin(\alpha_{\mathrm{R}}) =$$

$$= \left[\beta_{\mathrm{L}} \sin(\alpha_{\mathrm{L}}) + \beta_{\mathrm{R}} \sin(\alpha_{\mathrm{R}})\right] \Delta Z \tag{3}$$

which means that the relationship between the change Δd in disparity of the stereomicroscopic images and the move distance ΔZ of the motorized translation stage is linear for a certain stereomicroscope and each of its corresponding magnification.

The motivation to propose the method is that, whether an object in a microscopic image is clear or not is determined by whether it is in depth of field (DOF) or out of the DOF when the image is taken, and this is related to the distance between the object and the camera. Additionally, the distance is related to the disparity of the object in the stereoimage. Thus, if an appropriate distance range can be determined for each magnification of a stereomicroscope, the corresponding appropriate disparity range can also be determined. Then, with the help of the disparity information, the sharpness of arbitrary stereomicroscopic images can be judged. Moreover, if the image is not clear enough, the motorized translation stage T can be moved at that right place to capture a clear image according to the linear relationship between Δd and ΔZ.

2.2. Calibration of disparity range of clear stereomicroscopic image

The purpose of calibrating the disparity range of clear stereomicroscopic images is to use disparity as an index of sharpness of captured stereomicroscopic images, because disparity is inversely proportional to the distance between the object and the cameras of the stereomicroscope for imaging systems with parallel camera configuration. This calibration step only needs to be performed once for each magnification to obtain the disparity range with respect to clear stereomicroscopic images under the specific magnification.

It is assumed that a stereomicroscopic image exhibits the same sharpness when captured at the same height of the motorized translation stage. The advantage of the Tenengrad sharpness function has been previously verified for microscopic images [6]. Thus Tenengrad function values of the left (or right) view of a calibrated stereomicro-

scopic image sequence are calculated. Here we use the left view of this calibrated stereomicroscopic image sequence (herein-after referred to as "calibrated left microscopic image sequence"). Let $F_{T_1}, \ldots, F_{T_N}$ represent the Tenengrad function values of the calibrated left microscopic image sequence which are captured from blurry to clear and back to blurry again and N be the total number of images within the sequence. Then, the maximum $F_{T_{max}}$ is selected from F_{T_1} to F_{T_N}, and the corresponding calibrated left microscopic images sequence number S_{max} is recorded. According to the DOF range with respect to the specific magnification, the S_{max}-th image and $2n$ calibrated left microscopic images symmetrically surrounding the S_{max}-th image are selected as the clear images, that is, these $(2n + 1)$ images are taken within the DOF, and the image numbers of these $(2n + 1)$ images are recorded as the interval $[S_{CL}, S_{CR}]$, $1 \le S_{CL} < S_{CR} \le N$.

Then, the total N calibrated stereomicroscopic images are rectified to parallel calibrated stereomicroscopic images by employing the quasi-Euclidean epipolar rectification algorithm [12]. The matching points of a parallel calibrated stereomicroscopic image are found by using the speed up robust features (SURF) [13], and the disparity of the parallel calibrated stereomicroscopic image is calculated. Finally, by linear fitting the disparity and image number of the total N calibrated stereomicroscopic images, the disparity range $[d_{C,\,min}, d_{C,\,max}]$ with respect to the $(2n + 1)$ clear stereomicroscopic images is obtained and regarded as the disparity range of the clear stereomicroscopic image under the specific magnification, where $d_{C,\,min}$ and $d_{C,\,max}$ are the smallest and largest disparities of the clear stereomicroscopic images.

2.3. Capture of clear stereomicroscopic image

As mentioned above, it is difficult for traditional autofocusing methods to judge whether an arbitrary image captured with a monocular microscope is clear enough to satisfy the requirement if there is no other reference images. But for a stereomicroscope, the situation is different. In this paper, the sharpness judgment of an arbitrary stereomicroscopic image captured at a specific magnification is simplified as judging whether the disparity of the captured stereomicroscopic image is within the disparity range of a clear stereomicroscopic image or not. Moreover, if the captured stereomicroscopic image cannot satisfy the requirement, the move steps and direction of the step motor can be calculated by utilizing the linear relationship between the change in disparity of the stereomicroscopic image and the move distance of a motorized translation stage, so that the motorized translation stage can be moved to the focus position through several iterations.

Let d denote the disparity of an arbitrary stereomicroscopic image and r_d be the result of sharpness judgment. The judgment can be expressed as follows:

$$r_d = \begin{cases} 1 & \text{if } \; d \in [d_{C,\,min}, d_{C,\,max}] \\ 0 & \text{otherwise} \end{cases} \tag{4}$$

If the value of r_d is 1, it indicates that the corresponding stereomicroscopic image is clear; otherwise it is unclear.

Automatic movement to the focus position is performed according to the result of the sharpness judgment. Since the disparity range of clear stereomicroscopic images is calibrated symmetrically, the disparity at the focus position should be $d_{\mathrm{mc}} = (d_{\mathrm{C,\,min}} + d_{\mathrm{C,\,max}})/2$. Let the motorized translation stage move by height h (μm) when the step motor takes a step, and $d_{\mu\mathrm{m}}$ be the disparity of a micrometer (unit: pixel/μm). The disparity with respect to a move step d_{step} can be defined as $d_{\mathrm{step}} = d_{\mu\mathrm{m}} \times h$. Thus, the move steps and direction of the step motor can be determined according to the linear relationship between the change in disparity of a stereomicroscopic image and the move distance of a motorized translation stage, with which the motorized translation stage can be moved to the focus position. The move steps s_{mv} of the step motor are calculated by

$$s_{\mathrm{mv}} = \frac{d - d_{\mathrm{mc}}}{d_{\mathrm{step}}} \tag{5}$$

The move direction d_{mv} of the step motor is determined as

$$d_{\mathrm{mv}} = \begin{cases} 1 & \text{if} \quad s_{\mathrm{mv}} < 0 \\ 0 & \text{if} \quad s_{\mathrm{mv}} = 0 \\ -1 & \text{if} \quad s_{\mathrm{mv}} > 0 \end{cases} \tag{6}$$

when d_{mv} is 1, the motorized translation stage should be moved upward to reduce the distance between the object and the cameras; it is opposite when d_{mv} is –1. When d_{mv} is 0, it means that the motorized translation stage is just at the focus position, thus no movement is required.

Finally, the computer sends the two parameters s_{mv} and d_{mv} to a single-chip microcomputer (SCM) through serial communication, and the SCM controls the step motor such that the motorized translation stage performs the corresponding move to reach the focus position.

In summary, for a certain stereomicroscope, the disparity ranges of clear stereomicroscopic images are first calibrated for all magnifications by using series of clear and blurry stereomicroscopic images captured at each magnification, and the calibration procedure only needs to be implemented once. After that, during the imaging procedure, the disparity of a stereomicroscopic image captured at an arbitrary position is calculated and compared with the calibrated disparity range with respect to the same magnification of the stereomicroscopic image. If the disparity of the current stereomicroscopic image does not approximate to the clearest disparity, the move steps and direction of the step motor are calculated by employing the linear relationship between the change in disparity of a stereomicroscopic image and the move distance of a motorized translation stage. Then, a SCM will drive the step motor to adjust the motorized

translation stage to the focus position. The iterations are continued until the disparity satisfies the requirement which means that the clearest stereomicroscopic image is obtained.

3. Experimental results and discussions

3.1. Experiment platform

The experiment platform is composed of a digital stereomicroscope, motorized translation stage, SCM, and a computer. The digital stereomicroscope is a type of NSZ-800 produced by NOVEL Optics, and is with 1/2 inch CCD. The zoom multiple of objective is from 0.7× to 3×, and 0.7× is used in this paper. The resolution of a single view (left or right view) image is 720 × 576. A printed circuit board is placed on the motorized translation stage (CHUO SEIKI XA07A-R2H) as the object. The minimum move step of the motorized translation stage is 2 μm. The SCM is a type of 80C51 and controls the step motor to move the translation stage. The computer has an Intel Core(TM)i3 CPU at 3.19 GHz and 1.74 GB of memory.

3.2. Calibration of disparity range of clear stereomicroscopic image

In the experiments, 150 calibrated stereomicroscopic images are captured from blurry to clearest, and then from clearest to blurry. The interval of the height of the motorized translation stage of adjacent images is 10 μm. Figure 2 shows the left views of five of the calibrated stereomicroscopic images captured at different heights of the motorized translation stage.

The Tenengrad function values of the left views of the 150 calibrated stereomicroscopic images are shown in Fig. 3**a**. The values are fluctuant because the image contents are a little bit different in the visual field of the microscope and the Tenengrad function value is related to image content. However, the fluctuation does not change the tendency of the function. The sequence number $S_{\max}$ of the calibrated microscopic image with the maximum Tenengrad function value $F_{\mathrm{T}_{\max}}$ is 53. According to the DOF

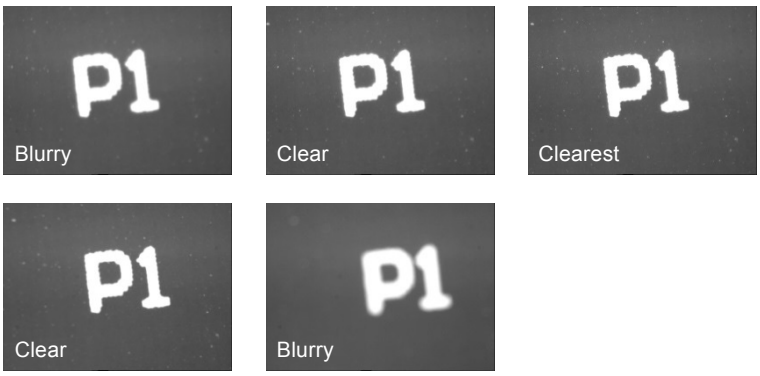

Fig. 2. Partial calibrated left views of stereomicroscopic image sequence.

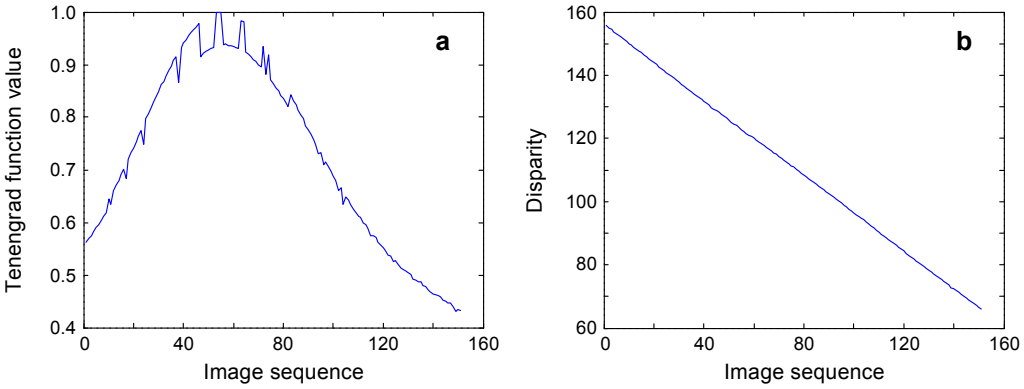

Fig. 3. Tenengrad function values of the left views of calibrated stereomicroscopic image sequence (**a**); disparities of calibrated stereomicroscopic image sequence (**b**).

of this magnification (300), n is selected as 15. Therefore, the image number of the $(2n + 1)$ calibrated clear stereomicroscopic images is from 38 to 68, that is, $[S_{CL}, S_{CR}]$ is [38, 68].

The disparities of all the 150 calibrated stereomicroscopic images are shown in Fig. 3**b**. It is seen that the disparity is linear with the image number. By linear fitting, the disparity and image number of the total 150 calibrated left stereomicroscopic images, the disparity range $[d_{C,\,min}, d_{C,\,max}]$ with respect to stereoimages whose image number is within $[S_{CL}, S_{CR}]$ is determined as [115.405, 133.100]. This calibration step can be performed only once because the disparity range is constant under the same magnification for a certain stereomicroscope.

3.3. Sharpness judgment of stereomicroscopic image

To test the performance of the proposed disparity servoing based fast autofocusing method, two types of stereomicroscopic images with different contents are used in this experimental step, as shown in Fig. 4, where the upper row shows the left view of the first type of four stereomicroscopic images captured at different heights of the motorized translation stage, and the lower row shows the left view of the second type of stereomicroscopic images.

According to the calibration method described in Section 2.2, disparities of all of the stereomicroscopic images captured for the calibration of the disparity range of clear stereomicroscopic images were calculated, the corresponding disparity range was determined, and the sharpness judgments of the eight images shown in Fig. 4 were also implemented. The results are given in Fig. 5. Alphabetical labels **a**–**h** in Fig. 4 are replaced by numerical labels 1–8 in Fig. 5. Figure 5**a** gives the sharpness judgment results. The vertical axis of Fig. 5**a** is disparity, the unit of which is pixel, and the two dash-dot horizontal lines indicate the disparity range of clear stereomicroscopic images. According to Eq. (4), the disparities of stereomicroscopic images in Figs. 4**a**, 4**b**,

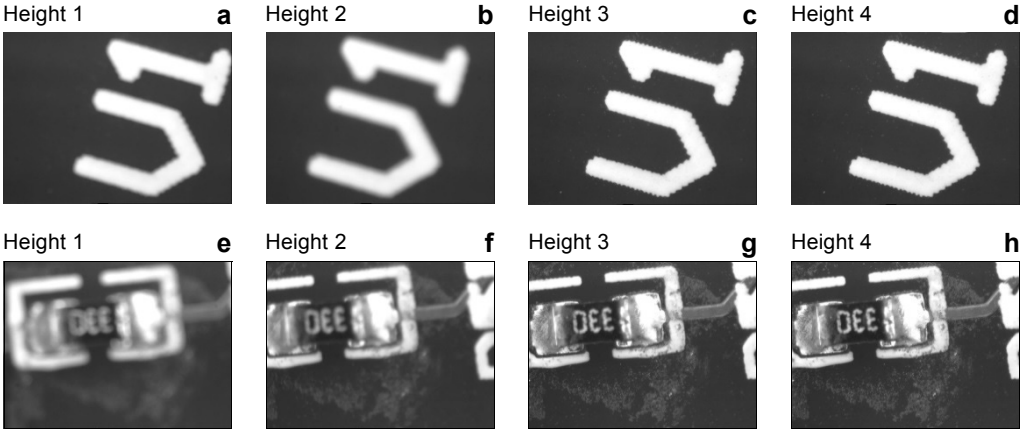

Fig. 4. Left view of stereomicroscopic test images (see text for explanation).

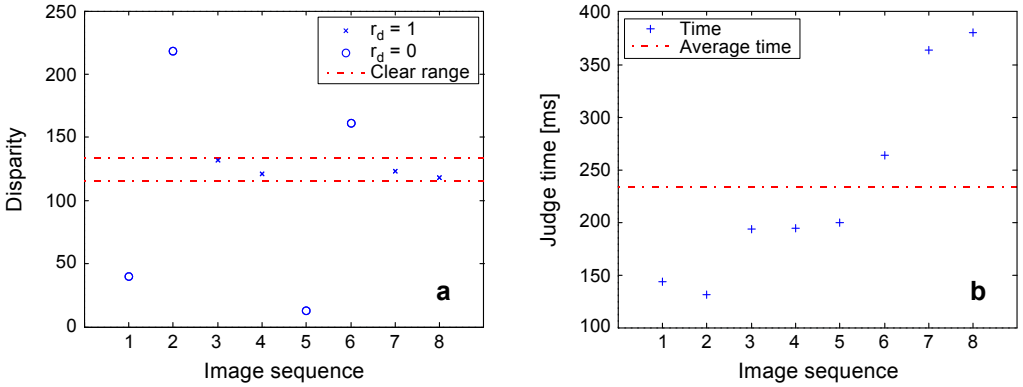

Fig. 5. Disparities and sharpness judgment results of stereomicroscopic test images (**a**); sharpness judgment time of stereomicroscopic test images (**b**).

4**e**, 4**f** are out of the clear disparity range, which means that these four stereomicroscopic images are blurred because they are captured out of the DOF. In contrast, the stereomicroscopic images shown in Figs. 4**c**, 4**d**, 4**g**, 4**h** are determined to be clear. The time of sharpness judgment for each stereomicroscopic image is also given in Fig. 5**b**. The average runtime is about 223 ms, as the dash-dot line indicated in Fig. 5**b**. It is seen that the time of sharpness judgment is low, because the proposed sharpness judgment method only needs fast disparity calculation and one numeric comparison operation. As mentioned above, traditional autofocusing methods cannot perform sharpness judgment for arbitrary stereomicroscopic images without a series of reference images, but the proposed method can do it fast and effectively. Moreover, it also lays a foundation for the following moving step of the motorized translation stage, and speeds up the entire autofocusing process.

3.4. Iterated move of motorized translation stage

With the sharpness judgment results and theory described in Section 2.3, the move step s_{mv} and move direction d_{mv} can be calculated. The computer then sends these parameters to the SCM to control the step motor that moves the translation stage. According to previous results, d_{mc} is calculated to be 124.253, and d_{step} to be 2. For the images shown in Fig. 4, the calculated s_{mv} and d_{mv} are listed in Table 1, from which the translation stage relative position can be inferred by comparing s_{mv} and d_{mv}. The distance between the translation stage current position and focus position is proportional to s_{mv}.

The real disparities of the first moved stereomicroscopic images are shown in Fig. 6**a**. The absolute difference between the actual disparity and the disparity with re-

T a b l e 1. Moving steps and direction of stereomicroscopic test image.

Index	1	2	3	4	5	6	7	8
s_{mv}	708	787	61	25	932	307	7	49
d_{mv}	1	–1	1	–1	1	–1	1	1

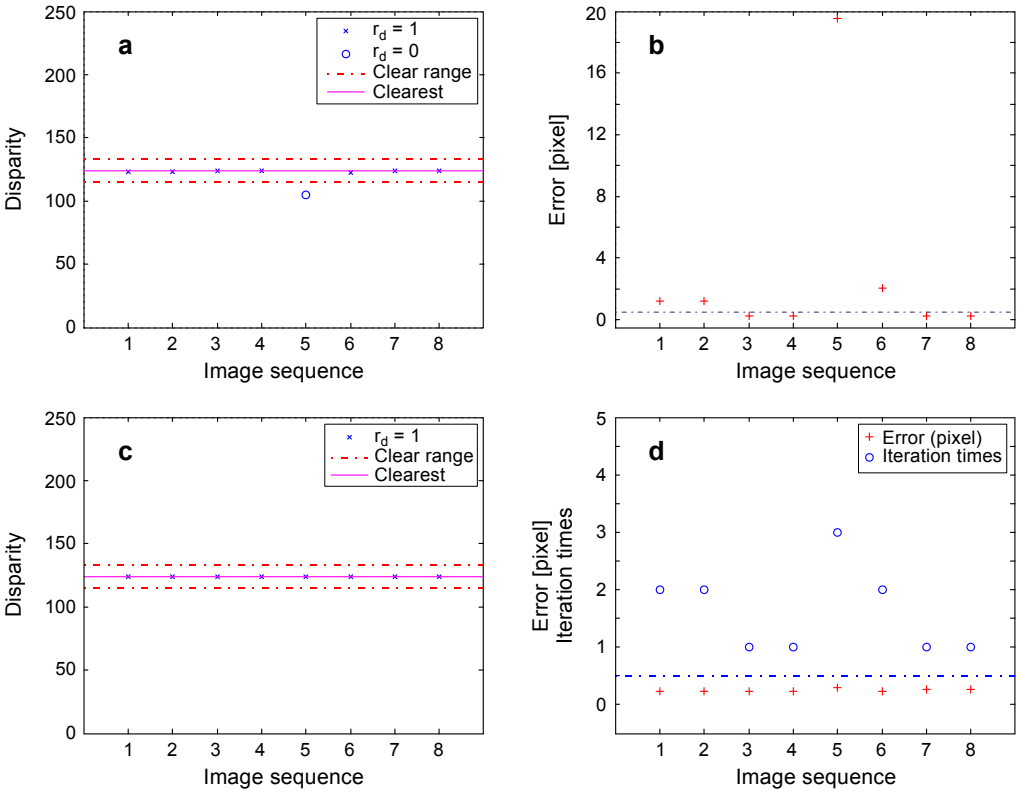

Fig. 6. Actual disparity of moved stereomicroscopic image (**a**); disparity error of moved stereomicroscopic image (**b**); actual disparity of iterated stereomicroscopic image (**c**); disparity error and iterations of iterated stereomicroscopic image (**d**).

spect to the focus position is given in Fig. 6**b**. According to Fig. 6**a**, the sharpness judgment results in Fig. 5**a** and the disparity error in Fig. 6**b**, the error between the disparity of the captured stereomicroscopic image after one move and the disparity with respect to the focus position is small (<0.3 pixel) if the r_d is 1 (*i.e.*, the image is judged to be clear). This is because the change in the clear disparity range is close to the ideal linear relationship. However, the error is large (about 19.5 pixel) if the r_d is 0. The reason is that the change in the non-clear disparity range belongs to an incompletely linear relationship due to the relatively inaccurate disparity calculation of blurry stereomicroscope images.

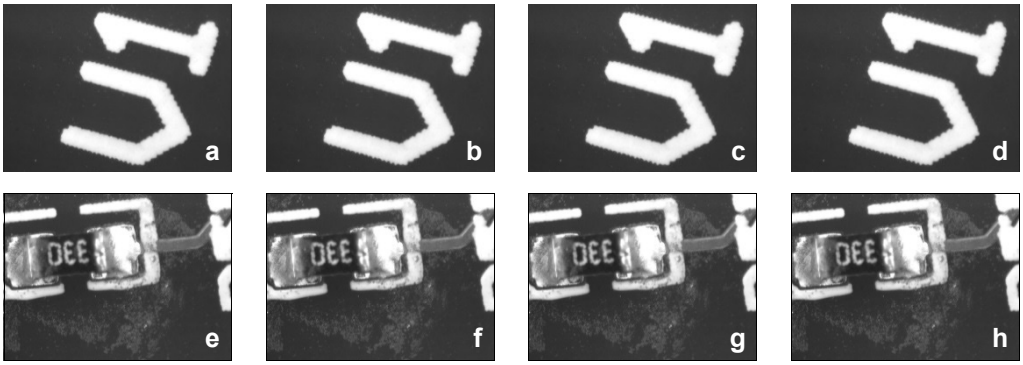

Fig. 7. Captured left microscopic image after iteration (see text for explanation).

To reduce the error between the actual disparity of the captured stereomicroscopic image and the disparity with respect to the focus position, the error threshold is set to 0.5, as shown by the dash-dot line in Fig. 6**b**. Then, the camera will automatically capture a stereomicroscopic image after moving translation stage, and the disparity will be calculated and compared time and time again until the error is less than the threshold. The final actual disparities of the stereomicroscopic images after iteration are shown in Fig. 6**c**. The final errors and iteration times are given in Fig. 6**d**. Further, the final captured images after iteration are shown in Fig. 7. From the iterated results in Figs. 6**c** and 6**d**, the final errors are within the preset threshold (<0.5 pixel), and only a small number of iterations are required. From Fig. 7, it is seen that the eight microscopic images are clear, and this demonstrates the effectiveness of the proposed disparity servoing based autofocusing method.

3.5. Time complexity comparison with traditional autofocusing method

For traditional autofocusing methods, let the time taken for the step motor move the motorized translation stage by one step be t_{move}, and the waiting time for capturing a stereomicroscopic image be t_{wait}. The time for calculating the sharpness function value can be neglected because it is much less than the above two times. Therefore, the autofocusing time of the traditional method is $(t_{\text{move}} + t_{\text{wait}})n_f$, when n_f is the number

of stereomicroscopic images captured for finding the clearest image, and the image sequence should be around the focus position symmetrically.

In contrast, the disparity range of a clear stereomicroscopic image just needs to be calibrated once for a certain microscope in the proposed method, so the corresponding time is not considered to the total autofocusing time. The main time of autofocusing of the proposed method consists of disparity calculation, sharpness judgment, iterated move, and the wait time for capturing a stereomicroscopic image at each of the iterations. Compared with the time of motorized translation stage move and wait, the other time is negligible. Since the entire move range is around the focus position symmetrically and the move direction can be determined by the proposed method, the step number of moves of the proposed method is half that of the traditional autofocusing method. Let the number of iteration be n_d, then the autofocusing time of the proposed method is $t_{\text{move}} n_f/2 + t_{\text{wait}} n_d$.

According to the traditional autofocusing method and the experimental iterated data in this paper, the times of waits for the traditional method are much greater than those for the proposed method, *i.e.*, $n_f \gg n_d$. For the experimental platform reported in this paper, t_{move} is 1 second and t_{wait} is 2 seconds. Therefore, the autofocusing time of the proposed method is about 1/6 that of the traditional method.

4. Conclusion

This paper proposes a fast autofocusing method for stereomicroscopes. Different from traditional autofocusing methods, the proposed method uses binocular image information. After the disparity range of the clear microscopic images is calibrated for each magnification of the stereomicroscope off-line, the disparity is selected as the sharpness index for arbitrary stereomicroscopic images and can enable fast autofocusing for the stereomicroscope. The proposed method also does not need plenty of experiments for selection of the optimal sharpness function, but only requires the fixed index for the calculations. Sharpness judgment for arbitrary stereomicroscopic images can be performed by utilizing the calibrated clear disparity range. The experimental results show that the translation stage can reach the focus position with a few times of iterations, thus saving a lot of autofocusing time.

Acknowledgements – This work is supported by the Natural Science Foundation of China under Grant No. 61271270, and the Natural Science Foundation of Zhejiang Province under Grant No. LY15F010005. It is also sponsored by K.C. Wong Magna Fund in Ningbo University.

References

[1] SHUNLI XIAO, YANGMIN LI, *Visual servo feedback control of a novel large working range micro manipulation system for microassembly*, Journal of Microelectromechanical Systems **23**(1), 2014, pp. 181–190.

[2] ÇELIK H.İ., DÜLGER L.C., TOPALBEKIROĞLU M., *Development of a machine vision system: real-time fabric defect detection and classification with neural networks*, The Journal of The Textile Institute **105**(6), 2014, pp. 575–585.

[3] CHUAN JIANG, MILLS J.K., *Development of a cell orientation control system for mouse embryo using electro-rotation*, 2014 IEEE International Conference on Mechatronics and Automation, 2014, pp. 1085–1090.

[4] SHAFAAT AHMED BAZAZ, NAYYER ABBAS, MUHAMMAD BILAL SAIF, NISAR AHMAD, *Design and characterization of MEMS based micrograsping system*, Assembly Automation **33**(3), 2013, pp. 260–271.

[5] CHAO-CHEN GU, KAI-JIE WU, JIE HU, CHENG HAO, XIN-PING GUAN, *Region sampling for robust and rapid autofocus in microscope*, Microscopy Research and Technique **78**(5), 2015, pp. 382–390.

[6] YU SUN, DUTHALER S., NELSON B.J., *Autofocusing algorithm selection in computer microscopy*, 2005 IEEE/RSJ International Conference on Intelligent Robots and Systems, 2005, pp. 70–76.

[7] XIN XU, YINGLIN WANG, XIAOLONG ZHANG, SHUNXIN LI, XIAOMING LIU, XIAOFENG WANG, JINSHAN TANG, *A comparison of contrast measurements in passive autofocus systems for low contrast images*, Multimedia Tools and Applications **69**(1), 2014, pp. 139–156.

[8] BARAN E.A., AYIT O., SANTIAGO V.B., LÓPEZ-DÓRIGA S., SABANOVIC A., *A self-optimizing autofocusing scheme for microscope integrated visual inspection systems*, Industrial Electronics Society, IECON 2013 – 39th Annual Conference of the IEEE, 2013, pp. 4043–4048.

[9] CHIEN-SHENG LIU, SHENG-HONG JIANG, *Precise autofocusing microscope with rapid response*, Optics and Lasers in Engineering **66**, 2015, pp. 294–300.

[10] CHIEN-SHENG LIU, YANG-CHENG LIN, PIN-HAO HU, *Design and characterization of precise laser-based autofocusing microscope with reduced geometrical fluctuations*, Microsystem Technologies **19**(11), 2013, pp. 1717–1724.

[11] MARTURI N., TAMADAZTE B., DEMBÉLÉ S., PIAT N., *Visual servoing-based approach for efficient autofocusing in scanning electron microscope*, 2013 IEEE/RSJ International Conference on Intelligent Robots and Systems, 2013, pp. 2677–2682.

[12] FUSIELLO A., IRSARA L., *Quasi-Euclidean epipolar rectification of uncalibrated images*, Machine Vision and Applications **22**(4), 2011, pp. 663–670.

[13] BAY H., TUYTELAARS T., VAN GOOL L., *Surf: speeded up robust features*, [In] *Computer Vision – ECCV 2006*, [Eds] A. Leonardis, H. Bischof, A. Pinz, Springer Berlin Heidelberg, 2006, pp. 404–417.

Received December 22, 2015
in revised form April 28, 2016